Lead-free piezoelectric ceramics: Alternatives for PZT?

Thomas R. Shrout · Shujun J. Zhang

Abstract Investigations in the development of lead-free piezoelectric ceramics have recently claimed comparable properties to the lead-based ferroelectric perovskites, represented by $Pb(Zr,Ti)O_3$, or PZT. In this work, the scientific and technical impact of these materials is contrasted with the various families of "soft" and "hard" PZTs. On the scientific front, the intrinsic nature of the dielectric and piezoelectric properties are presented in relation to their respective Curie temperatures (T_C) and the existence of a morphotropic phase boundary (MPB). Analogous to PZT, enhanced properties are noted for MPB compositions in the $(Na,Bi)TiO_3$-$BaTiO_3$ and ternary system with $(K,Bi)TiO_3$, but offer properties significantly lower. The consequences of a ferroelectric to antiferroelectric transition well below T_C further limits their usefulness. Though comparable with respect to T_C, the high levels of piezoelectricity reported in the $(K,Na)NbO_3$ family are the result of enhanced polarizability associated with the orthorhombic-tetragonal polymorphic phase transition being compositionally shifted downward. As expected, the properties are strongly temperature dependent, while degradation occurs through the thermal cycling between the two distinct ferroelectric domain states. Extrinsic contributions arising from domains and domain wall mobility were determined using high field strain and polarization measurements. The concept of "soft" and "hard" lead-free piezoelectrics were discussed in relation to donor and acceptor modified PZTs, respectively. Technologically, the lead-free materials are discussed in relation to general applications, including sensors, actuators and ultrasound transducers.

1 Introduction

In the past, innovations in actuators, sensors, and ultrasonic transducers have been the driving force for new developments in piezoelectric ceramics. Currently, the driving force is the result of environmental regulations[1]; hence, an enormous insurgence in the compositional development of lead-free piezoelectric materials.

$Pb(Zr_{1-x}Ti_x)O_3$ (PZT) and related perovskite compositions have been the mainstay for high performance actuators and transducers, owing to their superior dielectric, piezoelectric, and electromechanical coupling coefficients. Compositionally, PZT ceramics lie near a morphotropic phase boundary (MPB) separating tetragonal and rhombohedral phases, at $\sim x=0.48$ PT, shown in Fig. 1. MPB compositions have anomalously high dielectric and piezoelectric properties as a result of enhanced polarizability, arising from the coupling between two equivalent energy states, that is, the tetragonal and rhombohedral phases, allowing optimum domain reorientation during the poling process. Further modifications using acceptor and donor dopants give us the wide range of piezoelectric compositions we have today.

T. R. Shrout (✉) · S. J. Zhang
Materials Research Institute, Pennsylvania State University,
University Park, PA 16802, USA
e-mail: trs16@psu.edu

---

[1] For example: the legislation will be enforced in the EU as the draft directives on waste from electrical and electronic equipment (WEEE), restriction of hazardous substances (RoHS) and end-of life vehicles (ELV).
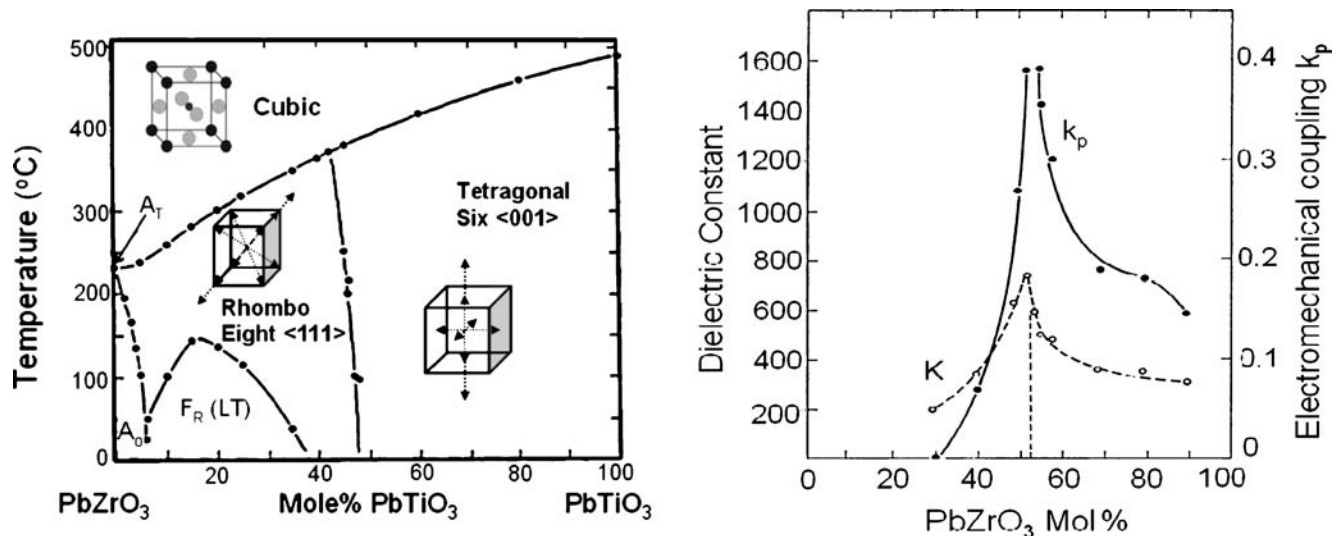
Fig. 1 Morphotropic phase boundary (*left*) and enhanced dielectric and piezoelectric properties (*right*) in the Pb(Zr,Ti)O$_3$ system. (after [1, 2]) MPB is defined as an abrupt structural change within a solid solution with composition. Note: The MPB is nearly temperature independent

Excellent reviews on piezoelectric ceramics, including both modified and undoped PZT ceramics, are given by Jaffe et al. [1, 2], and J. M. Herbert et al. [3, 4].

Recently, lead-free based piezoelectrics have been reported to offer comparable properties to that of PZT

ceramics, making them viable candidates for various applications [5–40]. In this paper, we present an overview of current developments in lead-free piezoelectric ceramics and contrast them to lead-based perovskite materials. Specifically, we discuss the "origin" of the enhanced

Table 1 Dielectric and piezoelectric properties of lead-free perovskite piezos "past and present".

Material	$\varepsilon_r/\varepsilon_0$	Loss	d_{33} (pC/N)	k_p	k_{33}	T_c (°C)	$T_{O–T}/T_d$ (°C)	Ref.
BaTiO$_3$	1,700	0.01	190	0.36	0.5	115	0	[40, 41]
BaTiO$_3$-CaTiO$_3$-Co	1,420	0.005	150	0.31	0.46	105	−45	[40, 42]
(K$_{0.5}$Na$_{0.5}$)NbO$_3$ (HP)	500	0.02	127	0.46	0.6	420		[45, 46]
(K$_{0.5}$Na$_{0.5}$)NbO$_3$	290	0.04	80	0.35	0.51	420	195	[47]
KNN-Li (7%)	950	0.084	240	0.45	0.64	460	~20	[6]
KNN-Li3%; Ta20% (LF3)	920–1,256	0.024–0.02	190–230	0.46–0.505	0.62	310–323	50–70	[6, 7]
KNN-LF4^a	1,570	/	410	0.61	/	253	25	[5, 13]
KNN-SrTiO$_3$ (5%)	950	/	200	0.37	/	277	27	[8, 9]
KNN-LiTaO$_3$ (5%)	570	0.04	200	0.36	/	430	55	[10]
KNN-LiNbO$_3$ (6%)	500	0.04	235	0.42	0.61	460	70	[11]
KNN-LiSbO$_3$ (5%)	1,288	0.019	283	0.50	/	392	45	[12]
NBT-KBT-LBT	1,550	0.034	216	0.401	/	350	160	[21]
NBT-KBT-BT	820	0.03	145	0.162	0.519	302	224	[43]
NBT-KBT-BT (MPB)	730	0.02	173	0.33	0.59	290	162	[43]
NBT-KBT-BT	770	0.034	183	0.367	0.619	290	100	[26]
NBT-BT	665	0.028	64 (d_{31})	0.28(k_{31})	/	/	/	[28]
NN-BT10%	1,000	0.015	147	/	/	235	/	[29]
NBT-KBT50%	825	0.03	150	0.22	/	320	210	[31]
SBT-KBT90	870	0.04	110	0.15	0.507	296	/	[43]
SBT-KBT85	1,000	0.05	120	0.16	0.491	250	/	[43]
BBT-KBT90	837	0.05	140	0.23	0.538	297	144	[43]
BBT-KBT80	630	0.04	95	0.15	0.361	290	238	[43]
Sr$_2$NaNb$_5$O$_{15}$^{a}	1,100	/	120	/	/	280	/	[44]

^{a} Textured ceramics; $T_{O–T}$: Orthorhombic to tetragonal phase transition; HP: Hot Pressed; NN: NaNbO$_3$; NBT: (Na$_{0.5}$Bi$_{0.5}$)TiO$_3$; KBT: (K$_{0.5}$Bi$_{0.5}$)TiO$_3$; LBT: (Li$_{0.5}$Bi$_{0.5}$)TiO$_3$; BT: BaTiO$_3$; SBT: (Sr$_{0.7}$Bi$_{0.2}$)TiO$_3$; BBT: (Ba$_{0.7}$Bi$_{0.2}$)TiO$_3$; KNN: (K$_{0.5}$Na$_{0.5}$)NbO$_3$; T$_d$: depolarization temperature.
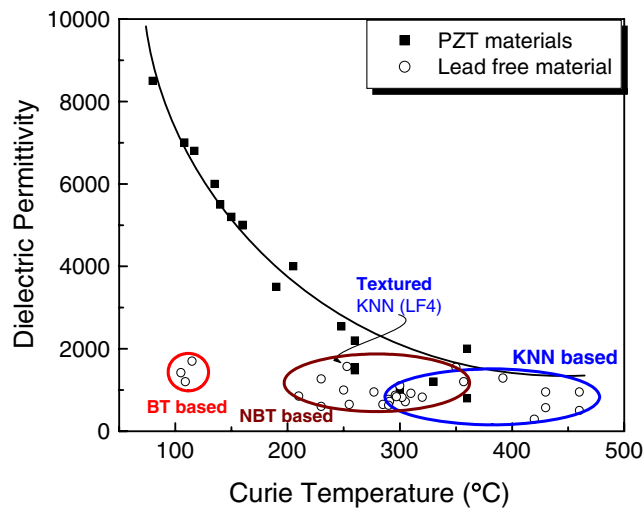
Fig. 2 Room temperature values of dielectric permittivity as a function of T_C for various piezoceramics

properties reported in relation to their underlying crystallographic structure relationships, that is, polymorphic phase transitions and morphotropic phase boundaries.

2 Background on piezoelectric ceramics

Among the important material parameters for piezoelectric ceramics, electromechanical coupling (k_{ij}), dielectric constant (K), or relative permittivity ε_r, and associated piezoelectric coefficients (d_{ij}) are key parameters. In general, the piezoelectric properties of a ferroelectric ceramic can be expressed using the simplistic term,

$$d_{ij} \sim 2Q_{ij}K\varepsilon_o P_i \tag{1}$$

where d_{ij} is the piezoelectric coefficient, P_i the remnant polarization on poling, K the dielectric constant, ε_o the permittivity of free space, and Q_{ij} the electrostriction coefficient. Since both Q_{ij} and P_i exhibit little dependence on composition or temperature below T_C in perovskite ferroelectric ceramics such as PZT, the piezoelectric coefficient d_{ij} and dielectric constant K are interrelated (i.e., a ceramic with high piezoelectric coefficient also exhibits a large dielectric constant). To achieve a high dielectric constant or piezoelectric coefficient, MPB-based ceramics are further engineered by compositionally adjusting the Curie temperature (T_C) downward relative to room temperature. A reduction in T_C, however, results in more temperature dependent properties and less polarization stability (i.e., aging and loss of piezoelectric activity). As a general rule of thumb, piezoelectric materials can be safely used to approximately $1/2$ T_C without significant reduction in piezoelectric activity. Therefore, not only must the dielectric and piezoelectric properties of a transducer

material be considered, but also the T_C and any polymorphic phase transition that may occur.

3 Lead-free piezoelectrics

Recent reports on lead-free piezoelectrics can be categorized into two main perovskite families: (1) $K_{0.5}Na_{0.5}NbO_3$ (KNN), and (2) $Na_{0.5}Bi_{0.5}TiO_3$ (NBT) [5–39]. Room temperature values of the dielectric, piezoelectric, and electromechanical properties have been compiled and tabulated in Table 1. In addition to the KNN and NBT families, properties for $BaTiO_3$-based piezoelectrics are also included [40–42]. Relaxor-based piezoelectrics of (Ba) $Sr_{0.7}Bi_{0.2}TiO_3$-$K_{0.5}Bi_{0.5}TiO_3$ [43] and tungsten bronzes [44], though included, will not be discussed owing to their relatively low properties.

For comparison with PZT materials, the room temperature values of K, d_{ij}, and coupling are plotted as a function of T_C and shown in Figs. 2, 3, and 4, respectively. As stated above, the dielectric and piezoelectric properties are intrinsically enhanced relative to a decrease in Curie temperature (T_C) for PZT-based materials, with only a modest (if any) enhancement noted for the three families of lead-free perovskites. In terms of the electromechanical coupling factors (k_p and k_{33}), no corresponding relationship with T_C for PZT or lead-free systems is observed.

Though $BaTiO_3$ was the first polycrystalline piezoelectric ceramic, its inherently low T_C and numerous polymorphic phase transitions limits its overall usefulness.

From the overview of the properties presented above, several questions arise. For the case of the KNN family, are the properties reported currently superior to that of the past? What is the origin of the enhanced properties that have been
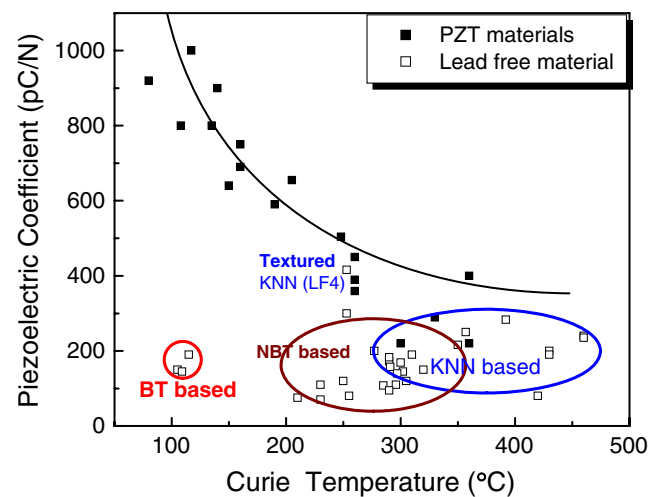

Fig. 3 Room temperature values of d_{33} as a function of T_C for various piezoceramics
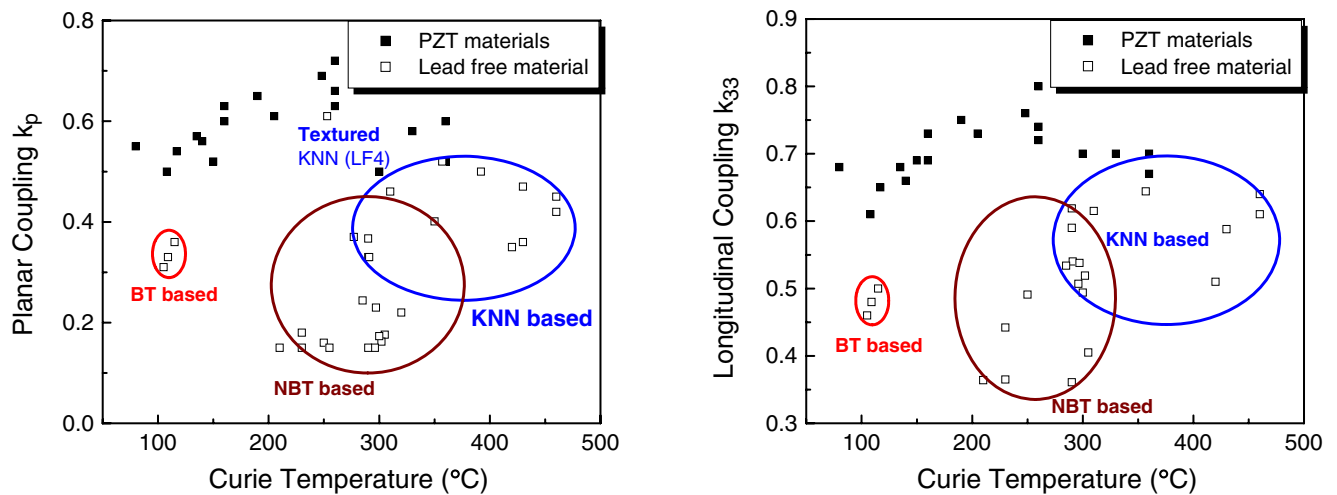
Fig. 4 Room temperature electromechanical coupling k_p (*left*) and k_{33} (*right*) for various piezoelectric ceramics. (The data in Figs. 2, 3, and 4 are obtained from [2, 5–54])

widely reported? For the KNN and NBT families, are the T_C's reported valid in relation to temperature usage range? From a technological perspective, are there distinct families of "soft" and "hard" lead-free piezoelectrics? Finally, how the lead-free piezoelectrics "stack up" against PZT in various applications?

4 (K$_{0.5}$Na$_{0.5}$)NbO$_3$ system: past and present

The phase diagram for the solid solution $(1-x)$KNbO$_3$–(x) NaNbO$_3$ system is given in Fig. 5. Reported in 1955, a

morphotropic phase boundary was identified at x~0.5 separating two orthorhombic ferroelectric phases. Inherent to MPBs, a maximum in remnant polarization (P_r) and minimum in coercive field (E_c) were reported [45]. A broad maximum in the planar coupling coefficient was observed, however, with no enhancement in the dielectric properties for either air-fired or hot pressed materials, see Fig. 5b. Table 2 presents dielectric and piezoelectric data for KNN with MPB compositions, reported prior to 1962 and for material recently processed using "optimal" processing and various fluxes. As presented, no significant differences in the piezoelectric properties are observed.
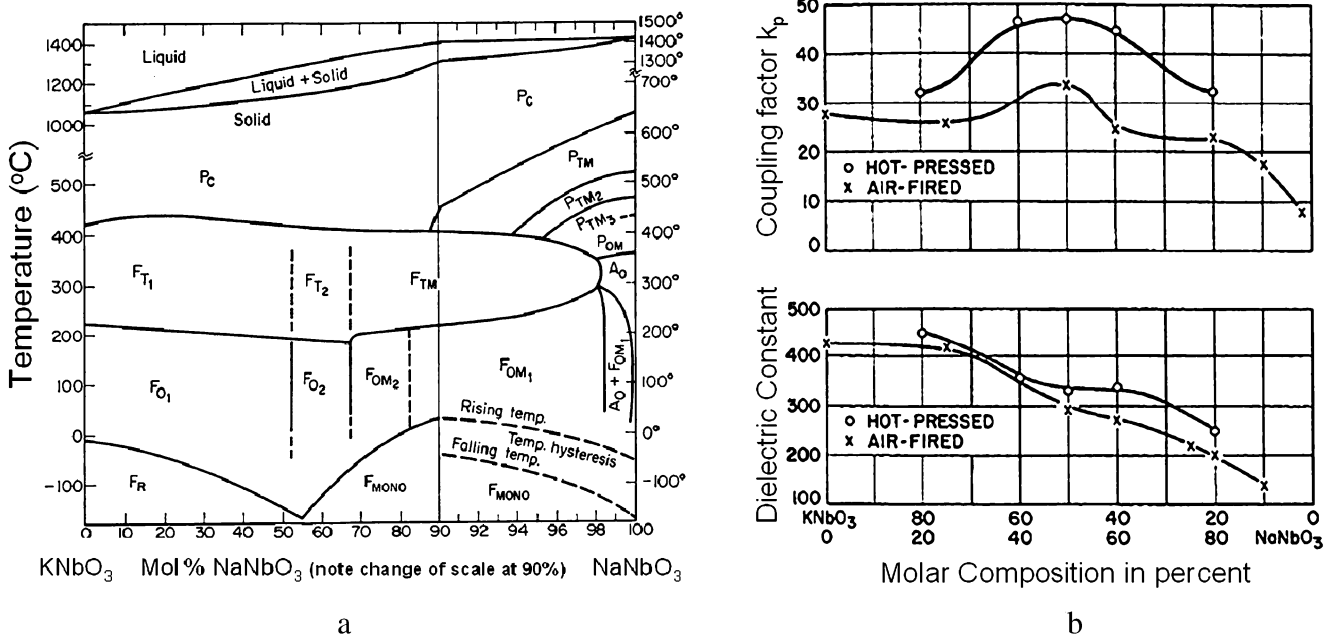

a

b

Fig. 5 Phase diagram for the KNbO$_3$-NaNbO$_3$ system (**a**) (after [1]) and dielectric and piezoelectric properties as a function of composition (**b**) (after [45]) Note: the orthorhombic–orthorhombic MPB is at ~50 mol% NaNbO$_3$

Table 2 Dielectric and piezoelectric properties of KNN ceramics: "past" and "present".

Properties	Air–fired 1959 [47]	Hot Pressed 1962 [45]	Standard 2005–2006 [16, 48, 52]	CuO flux 2005 [16]	KCT/KCN Flux 2005 [17, 18]	ZnO Flux 2006 [52, 54]
ε_r	290	490	429–605	231	250	500–650
d_{33} (pC/N)[a]	80	127	98–107	86	90(High Field-190)	117–123
k_p	36%	~46%	33.4–40%	37.8%	41%	0.4–0.44

[a] Comment: Berlincourt d_{33} values obtained on soft piezoelectric ceramic disks are generally higher (~10–20%) than values obtained using the IEEE Standards [55, 56].

It is important to note, KNN material prepared by spark plasma sintering reported significantly higher dielectric and piezoelectric properties than those given in Table 2, with $\varepsilon_r\sim700$ and $d_{33}\sim148$ pC/N [49, 50]. It is suggested that the enhancement is the result of extrinsic contributions to the polarizability associated with submicron grain sizes, similar to that found in fine grain $BaTiO_3$ [51], warranting further investigations.

5 Enhanced properties: morphotropic phase boundary versus a polymorphic phase transition

Analogous to PZT, a morphotropic phase boundary separating ferroelectric tetragonal, and rhombohedral phases exists in the $Na_{0.5}Bi_{0.5}TiO_3$-$BaTiO_3$ and related ternary system with $K_{0.5}Bi_{0.5}TiO_3$ [32] (the former shown in Fig. 6a). Both the dielectric and piezoelectric properties are significantly enhanced, as evident in Fig. 6b. Unlike

that of the PZT system, the MPB is strongly curved, and prior to the prototypic cubic transformation, a phase transformation to an anti-ferroelectric phase occurs, as shown in Fig. 7. The consequence of this transformation is a loss of polarization and thus piezoelectric activity. Figure 8 shows pyroelectric data for BNBK79 and BNBK88 ceramics, reflecting that the temperature of depolarization (T_d) is significantly lower than T_C for compositions in these systems. It is also confirmed by the electromechanical behavior of the BNBK system in Fig. 9, where the materials were found to be depoled at T_d. The T_d values for various BNBK compositions are listed in Table 1.

For the KNN family, reports of enhanced dielectric and piezoelectric properties were attributed to a morphotropic phase boundary separating orthorhombic and tetragonal phases [5–11]. Though technically a MPB, the enhancement in properties is a result of compositionally shifting the T_{O-T} polymorphic phase transition downward to room temperature. As first reported in $BaTiO_3$ [1, 58], and later
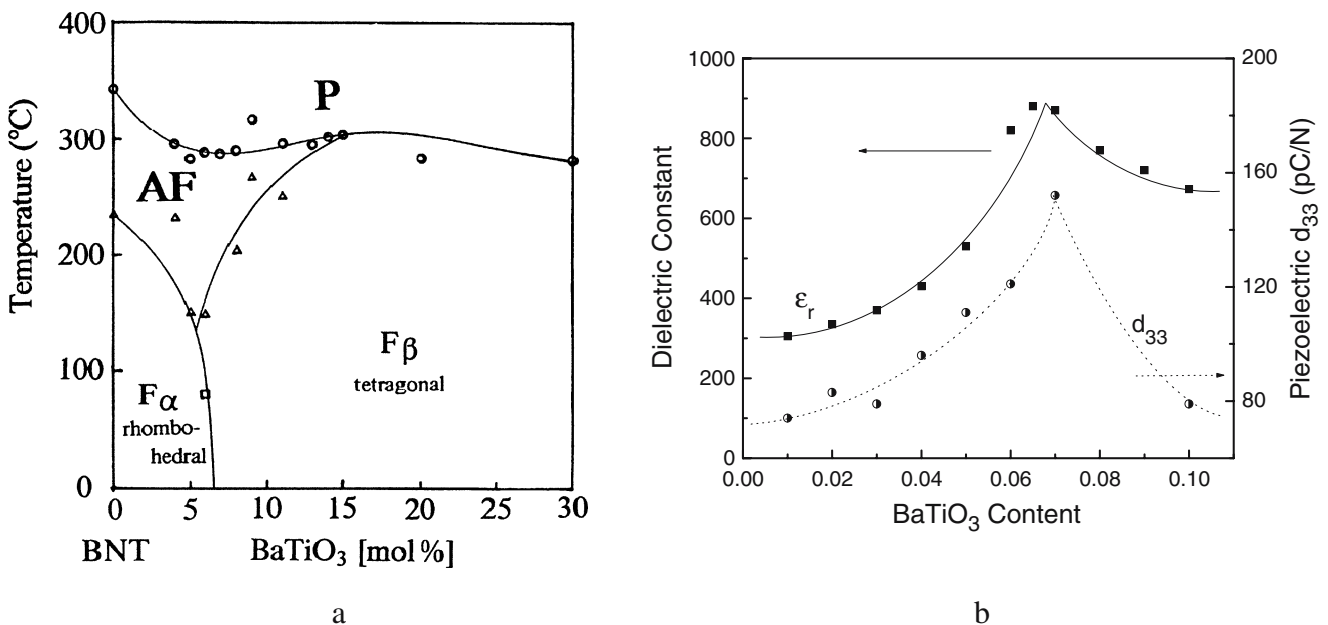

Fig. 6 Phase diagram for NBT-BaTiO₃ (**a**) (after. [32]) and temperature behavior (**b**) (data obtained from [33]) AF: Anti-ferroelectric; P: Paraelectric Cubic Phase
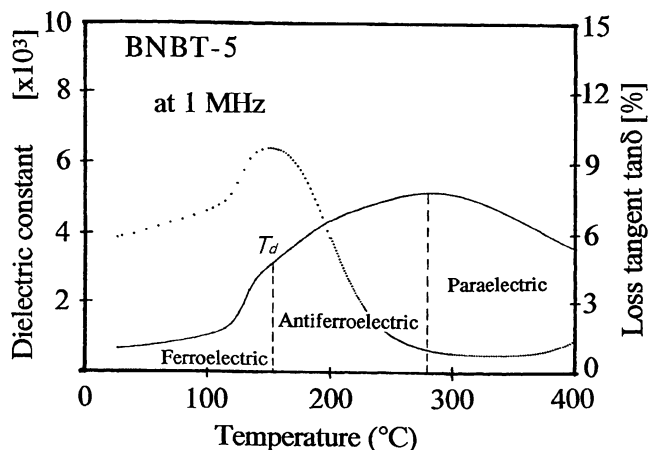
Fig. 7 Phase transformation in the NBT-BT system (after [32])

morphic phase transition. The enhancement in piezoelectricity is clearly evident in Fig. 13, where maxima in both coupling coefficient and piezoelectric d_{31} are again found at the T_{O-T} for two representative KNN compositions.

Figure 14 presents the phase diagram of the KNN system as a function of compositional modifications, including LiTaO$_3$, LiNbO$_3$, and SrTiO$_3$ [8–11], in which T_{O-T} can be readily shifted from ~200 °C for pure KNN to room temperature with ~5 mol% additions. Similar phase diagrams and their compositional temperature dependence on the various polymorphic phase transitions are well documented for KNbO$_3$-KTaO$_3$ [1, 61] and BaTiO$_3$ [1, 58], the latter being the underlying basis for the development of temperature stable ceramic capacitors.

From the above, it is evident that the temperature dependence of a polymorphic ferroelectric–ferroelectric phase transition mimics the compositional dependence of properties for a true MPB. In addition to strong temperature dependent behavior, thermal cycling between two distinct ferroelectric phases is expected to result in a reduction in polarization. Figure 15 gives the electromechanical coupling k_{31} of a KNN-LS system as a function of thermal cycling. Following the initial cycle, k_{31} decreased by nearly 10% at room temperature, ultimately stabilizing after several thermal cycles. The decrease in properties is clearly the result of cycling through regions of distinctly different domain states. As a point of future investigations, the degree of degradation may be correlated to the specific state at which the poling took place.

Presented in Fig. 16, a maximum in P_r is evident at the T_{O-T} polymorphic phase transition near room temperature, analogous to a MPB composition. This maximum in P_r is expected owing to the summation of possible crystallographic orientations, with 12 <110> spontaneous polariza-

in KNbO$_3$ [1, 57], the enhanced polarizability associated with a polymorphic phase transition leads to maxima in the dielectric and piezoelectric properties. This behavior is clearly shown for the case of Cd modified NaNbO$_3$ [1, 60] and pure KNbO$_3$ [1, 57] in Figs. 10 and 11, respectively. As shown, maxima occurred at all the ferroelectric–ferroelectric polymorphic phase transitions, with the highest levels of piezoelectric activity belonging to the orthorhombic-tetragonal transition.

Figure 12 gives the dielectric permittivity and dielectric loss for a modified KNN over the temperature range of −50–450 °C. As shown, two dielectric anomalies are presented with the T_c~380°C belonging to the tetragonal-cubic phase transition and the anomaly at room temperature being associated with the orthorhombic–tetragonal (T_{O-T}) poly-
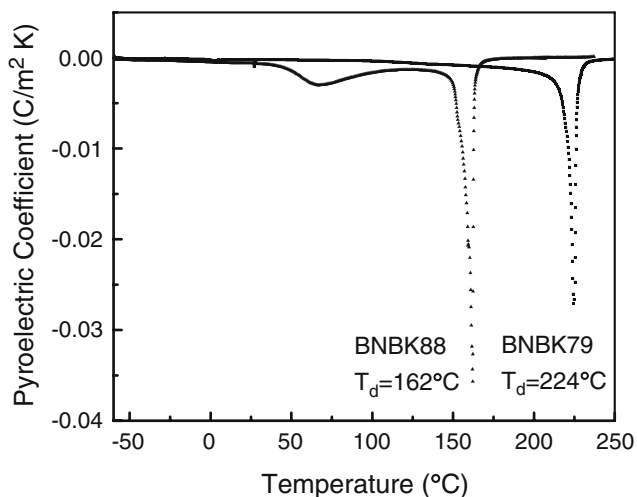

Fig. 8 Depolarization (T_d) temperature of two compositions in the NBT-KBT-BT system, as determined by pyroelectric measurements (after [59])
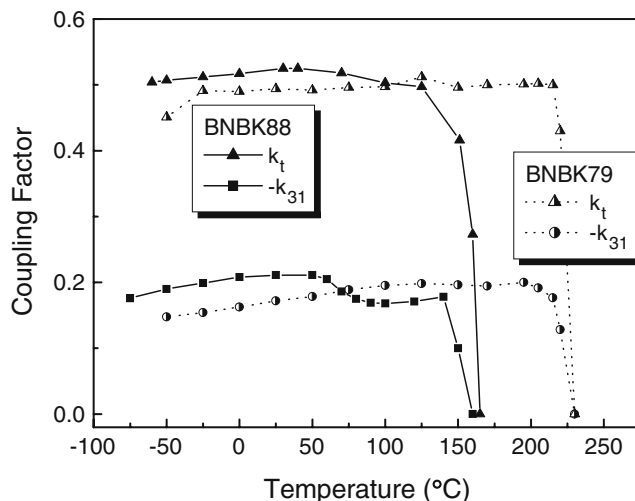

Fig. 9 Temperature dependence of electromechanical coupling factors k_t and k_{31} for BNBK79 and BNBK88 ceramics (after [59])
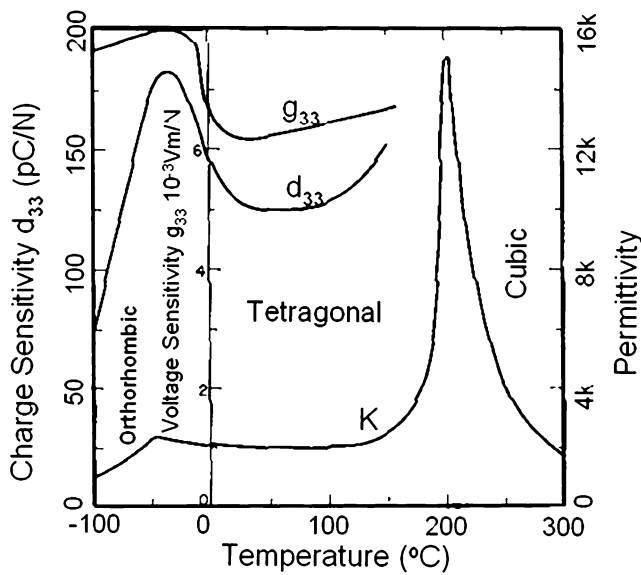
Fig. 10 Dielectric constant and piezoelectric coefficient versus temperature for $Na_{0.75}Cd_{0.125}NbO_3$ (after [1])

Fig. 12 Dielectric permittivity as a function of temperature for a KNN-LS5% material (after [62])

tion directions for an orthorhombic phase and six <001> directions for a tetragonal phase. However, at this time, it is difficult to explain the maximum in E_C, which generally reaches a minimum near a MPB. The decrease of E_C with increasing temperature can be explained by the fact that the domain wall motion and polarization reversal becomes easier with increasing temperature, a thermally activated process. Additional aspects that distinguish a polymorphic based piezoelectric and/or based on MPB will be discussed in later sections.
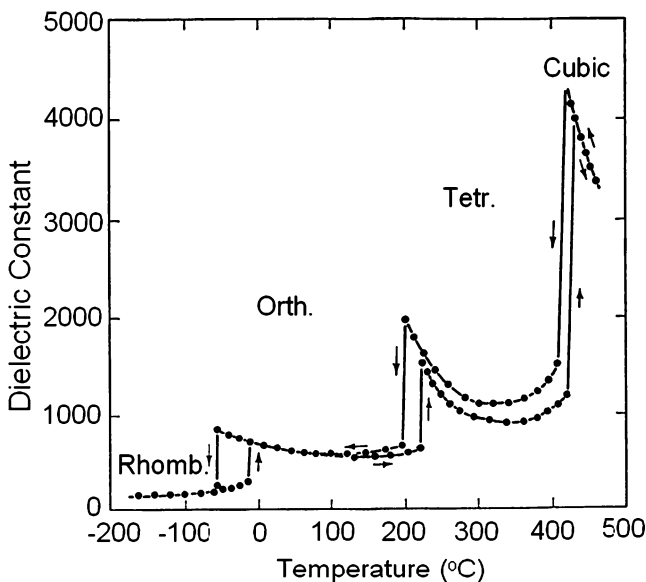
6 "Soft" and "hard": PZT piezoelectrics

The diversity of piezoelectric applications has led to the development of an extensive array of modified PZT and related ceramics. Generally, based near the MPB, the substitution of small amounts of cations (1–2 mol%) modifies the dielectric and piezoelectric properties. Doping with cations with a low valence, e.g. Fe^{+3} replacing Ti^{+4}/Zr^{+4} or K^{+1} for Pb^{+2}, results in oxygen vacancies, subsequently resulting in re-orientable dipoles that align in the direction of the polarization vector within domains, creating internal fields that stabilize the domain configuration and reduce domain wall mobility. This hardening effect results in a reduction in dielectric constant and loss and piezoelectric activity while the coercive field (E_C) and mechanical Q

Fig. 11 Dielectric constant versus temperature for $KNbO_3$, showing the various polymorphic phase transitions (after [1, 57])

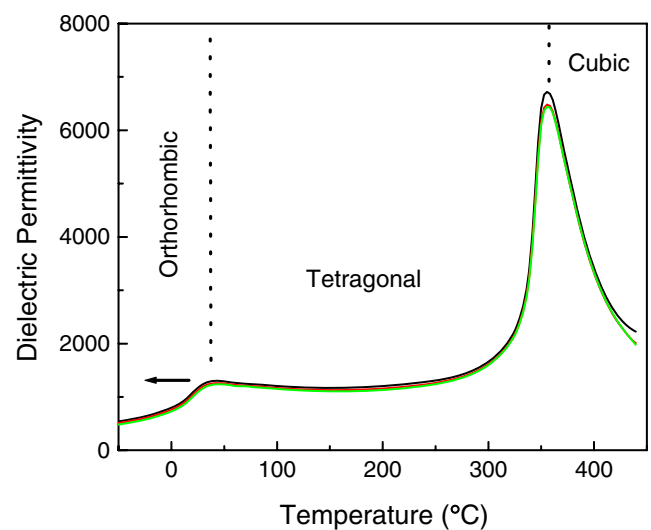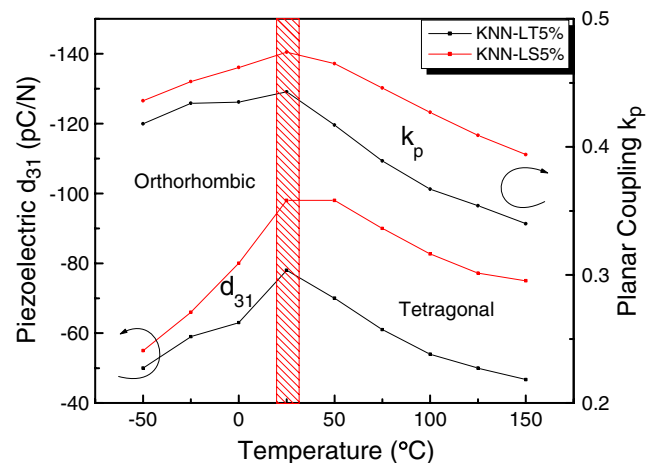**Fig. 13** Piezoelectric coefficient and coupling factor as a function of temperature for $LiTaO_3$ (LT) and $LiSbO_3$ (LS) modified KNN systems (after [62])

(inverse of mechanical loss) increase. In addition, the electrical resistivity of acceptor doped PZTs is reduced. This more stable behavior makes them suitable for high power and high voltage applications. Typical values of the dielectric and piezoelectric properties for two classes of "hard" PZT, DoD Type I and III, are given in Table 3 [2, 64, 65]. A representative P/E (polarization versus electric field) behavior is shown in Fig. 17 (left), where the off-set in coercive field reflecting the level of internal bias is clearly shown [66]. It is this development of internal bias that effectively increases the coercive field of hard piezoelectrics.

Donor doping of PZT results in the opposite effect of acceptor modified piezoelectrics, with dielectric and piezo-electric activity increasing, while the coercive field and mechanical Q decrease. This change is the result of lead vacancies arising from the replacement of Pb^{+2} with cations such as La^{+3} and/or Nb^{+5} for Ti^{+4}/Zr^{+4}, enhancing the mobility of domain walls. Though the dielectric loss increases, the electrical resistivity significantly improves, allowing operation at relatively high temperatures. The donor doped materials are in general both electrically and mechanically "soft". This family of piezoelectrics is generally used for medical ultrasound transducers, pressure sensors, and actuators, offering high resistivity and piezo-electric coupling. Typical values of DoD Type II and VI, "soft" piezoelectrics, are given in Table 3 [2, 64, 65]. The P/E behavior for a "soft" piezoelectric is shown in Fig. 17 (right).

Isovalent substitutions, such as Sr^{+2} and Ba^{+2} for Pb^{+2} and Sn^{+4} for Ti^{+4}/Zn^{+4}, are used to shift the Curie temperature downward, intrinsically enhancing the dielectric and piezo-electric properties, as presented earlier in Figs. 2 and 3. The Type VI piezoelectric is a good example of an isovalent
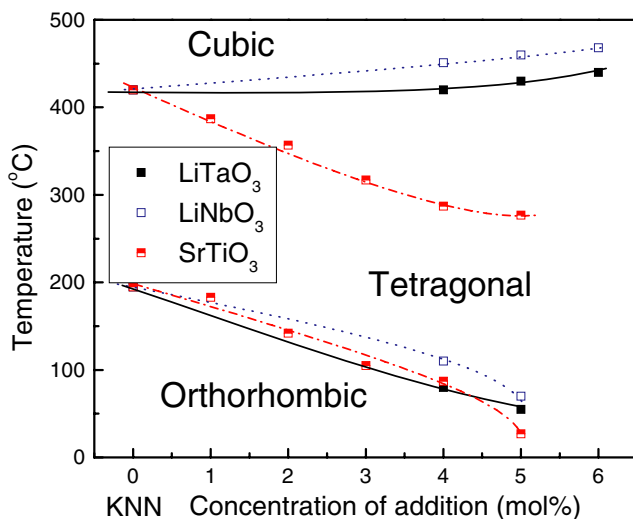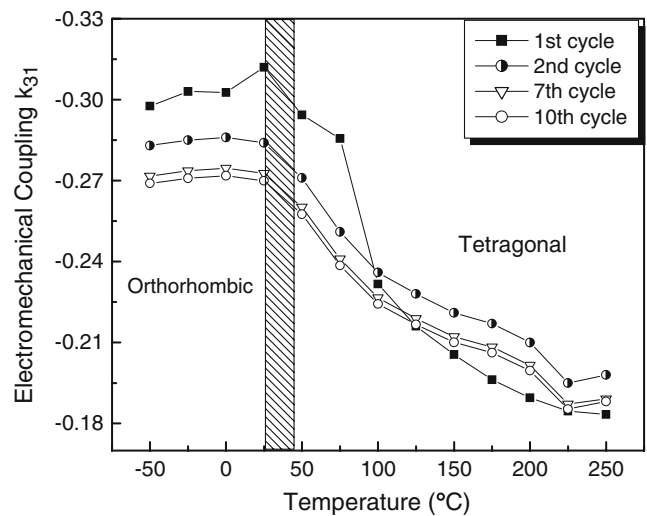
Fig. 15 Electromechanical coupling factor k_{31} as a function of temperature for KNN-LS as a function of thermal cycling (after [63])

modified PZT, with a greatly reduced T_C. With decreasing T_C, both E_C and P_r are reduced accordingly.

Excellent reviews of the effects of "acceptor" and "donor" doped PZTs and effects on properties are described in [1, 2, 64, 65].

7 "Soft" and "hard": lead-free piezoelectrics

Before the discovery of MPB PZT, compositional mod-ifications to $BaTiO_3$ were widely established. Reviewed by Jaffe [1], most modifications result in a thermal shift of the various polymorphic phase transitions underlying the change in properties. For example, modifications with
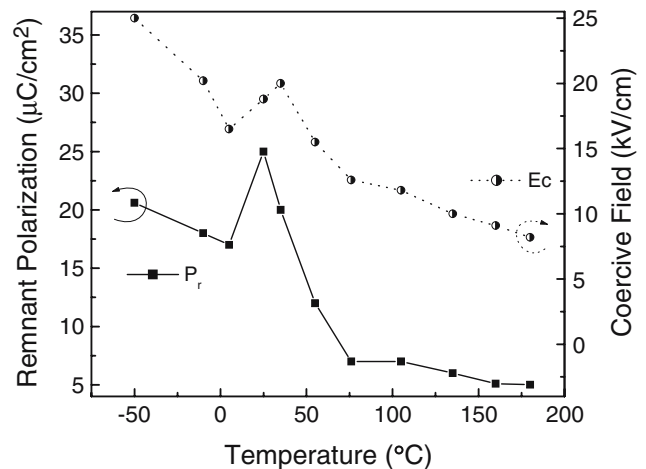
Fig. 14 Phase diagram for modified KNN (data from [8–11]) Note: $BaTiO_3$ additions are analogous to $SrTiO_3$ [9]

Fig. 16 Remnant polarization and coercive field as a function of temperature for KNN-LS (after [63])

Table 3 Detailed properties for "hard" and "soft" PZT materials.

Material	T_C (°C)	ε_r	Loss	k_{33}	d_{33} (pC/N)	d_{33}^*	g_{33} (10^{-3} Vm/N))	E_C (kV/cm)	Q
DoD I PZT4	328	1300	0.004	0.7	290	(330)	25	~18	>500
DoDII PZT5A	365	1700	0.02	0.71	375	(600)	25	~15	75
DoDIII PZT8	300	1000	0.004	0.64	225	(250)	25	~22	>1000
DoDVI PZT5H	190	3400	0.02	0.75	590	(800)	20	6–8	65

* d_{33} values determined at a field of 20 k V/cm; the level of internal bias for "hard" PZT ranged from 3–10 kV/cm

$CaTiO_3$ result in shifting the T_{R-O} and T_{O-T} polymorphic phase transitions downward while maintaining T_C, resulting in a piezoelectric with improved temperature stability. Analogous to acceptor doped PZTs, $BaTiO_3$ modified with cations, such as Co^{3+} and $Mn^{2+,3+}$, increase mechanical Q while decreasing dielectric loss. Overall, however, the low T_C and properties are significantly lower than PZT, limiting their usefulness in today's applications.

For the KNN family, unmodified compositions exhibit "soft" like behavior, with high loss, low mechanical Q, and modest $E_C \sim 5$–9 kV/cm. Properties affected by modifications to date have been primarily the result of enhanced densification as with additions of ZnO, SnO_2, Sc_2O_3, acting as fluxes with minor changes in both T_C and T_{O-T} [52, 54]. The addition MnO_2, generally used as an acceptor dopant, resulted in reduced grain growth, however, no evidence of "hardening" was observed [15].

The addition of CuO (and/or KCuTaO, KCuNbO) flux, however, did result in a "hardening" effect, as reported in Ref [16–18]. The incorporation of Cu^{+1} cations onto the B-site, replacing Nb^{+5}, would act as an acceptor dopant. From the properties summarized in Table 4, the dielectric and piezoelectric properties were reduced, while mechanical Q and dielectric loss increased and decreased, respectively.

For the orthorhombic–orthorhombic MPB based compositions of KNN modified with the T_{O-T} engineered to near room temperature, "soft" like behavior is noted. From Table 4, we see mechanical Q values are about 40–50, with dielectric loss on the order of a few percent, typical of a soft material. However, from Fig. 18, E_C values of >15 kV/cm are more indicative of hard piezoelectrics, and interestingly significantly higher than pure and acceptor modified KNN. Attempts to introduce vacancies in modified KNN with Sr^{+2} or Ba^{+2} ions on the A-site and Ti^{+4} replacing Nb^{+5} on the B-site, resulted in little effect on the dielectric and piezoelectric properties [37]. As with $BaTiO_3$ based piezoelectrics, changes observed were the result of a shift in the polymorphic phase transition and grain size effects. It should also be noted that a "pinched" polarization hysteresis was observed for thermally cycled samples, as shown in the small insert in Fig. 18, analogous to a "hard" PZT material, with an internal bias of 5 kV/cm. The "pinched" behavior could be eliminated when the sample was heated up to 100 °C.

In the BNBK family (unmodified), the P/E loops, see Fig. 19, exhibit E_Cs significantly higher than that of the hardest MPB PZTs, with E_Cs~30 kV/cm. However, they exhibit dielectric loss and mechanical Q values reflective of "soft" materials, as reported in Table 4. Attempts to
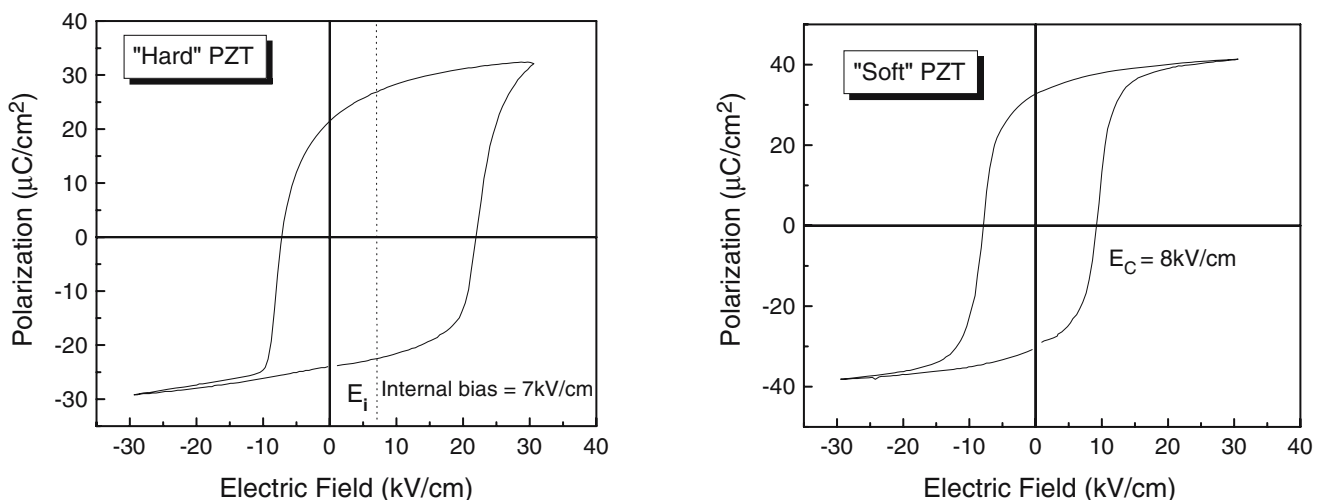

Fig. 17 Polarization hysteresis for "hard" PZT (*left*) and "soft" PZT (*right*)

Table 4 Detailed properties for BT, KNN and BNBK based lead-free materials.

Material	T_C (°C)	T_{O-T}/ T_d (°C)	ε_r	Loss	k_{33}	d_{33} (pC/N)	d_{33}^*	g_{33} (10^{-3} Vm/N))	E_C (kV/cm)	Q
BaTiO$_3$	115	/	1,700	0.01	0.50	190	/	13	1–2	300
BT-CT-Co	109	/	1,420	0.005	0.46	150	190	12	7	800
KNN (HP)	420	195	496	0.02	0.61	127	/	29	~5	240
KNN-Cu	414	180	231	0.003	0.38 (k_p)	86	85	42	/	2,280
KNN-KCT	385	190	250	0.004	0.42 (k_p)	90	180	40	9	1,300
KNN-LS	368	35	1,380	0.02	0.62	260	360	20	~18	40
KNN-LT	323	60	1,256	0.016	0.51(k_p)	230	320	21	/	73
BNBK79	280	224	650	0.04	0.54	135	180	24	37	110
BNBK88	262	162	810	0.02	0.60	170	210	24	29	150

$x(Na_{0.5}Bi_{0.5})TiO_3 - y(K_{0.5}Bi_{0.5})TiO_3 - zBaTiO_3 [x + y + z = 1 ; y : z = 2 : 1]$–BNBK100x
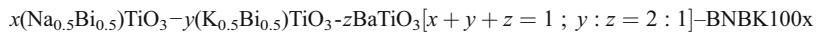
modify the BNBK type materials with dopants have been limited. Isovalent additions including La^{+3} have reported only modest changes in properties [67–69], being associated with enhanced densification and a downward shift in the ferroelectric–antiferroelectric (T_d) phase transition. A decrease in E_C was associated with downward shift in T_d. A significant decrease in E_C and T_d was also reported for CeO$_2$ doped BNBK, however, with a modest "hardening" effect, with mechanical Qs increasing from ~40 to 110 [27].

8 Extrinsic response

In addition to the piezoelectric activity of the crystallographic contribution in ferroelectric materials, their domains react to an applied electrical and/or mechanical field, adding to the piezoelectric response. This extrinsic effect arises primarily from domain wall contributions, although additional contributions can occur, such as grain boundary effects and displacement of inter-phase boundaries [66]. This extrinsic effect can be clearly seen for a "soft" PZT in Fig. 20, where a highly non-linear–strain-electric field behavior is observed. As compared to a "hard" PZT, the strain–electric field behavior is accompanied by hysteresis (the strain hysteresis is calculated by $\Delta x/x$ in which Δx is the width of the widest part of the loop and x is the peak strain [70]). For the case of PZT type II and VI piezoelectrics, strain hysteresis reaches levels on the order of 25% at fields of ~25 kV/cm, resulting in effective d_{33}^* 30–60% higher than the low field values, see Table 3. Interestingly, similar levels of hysteresis and enhanced d_{33} are found for the KNN and BNBK based lead-free materials. As shown in Fig. 21, the high field piezoelectric d_{33}^* is about 30–50% higher than the low field values.
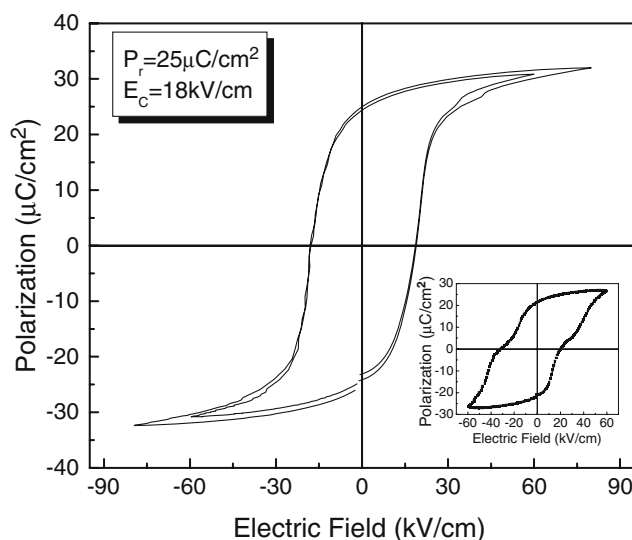
Fig. 18 Polarization hysteresis for modified KNN ceramic (after [63])
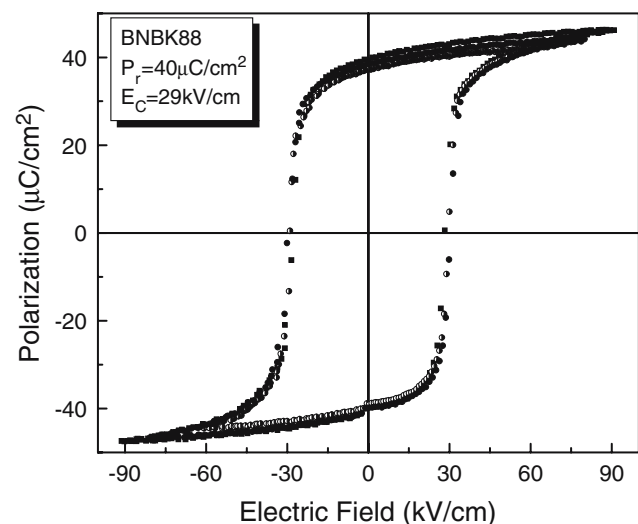
Fig. 19 Polarization hysteresis for BNBK88 with MPB composition (after [59])
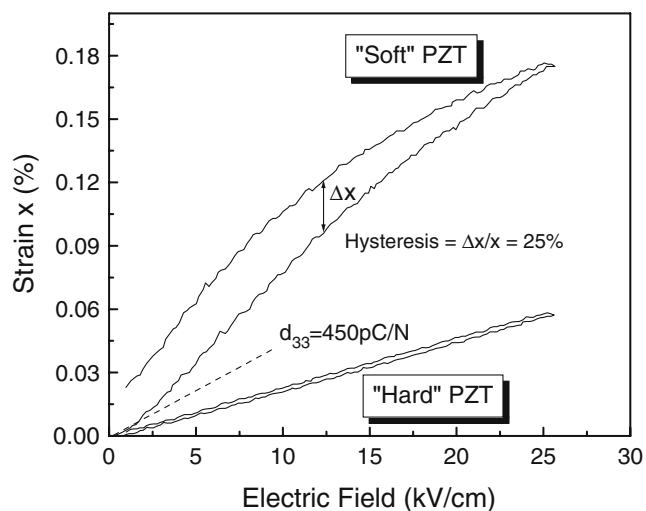
Fig. 20 Strain versus electric field for a "soft" and "hard" PZT, showing respective levels of hysteresis

Figure 22 shows that the high levels of strain- E field hysteresis occurs over the entire usage temperature range for both modified KNN and BNBK. The strongly temperature dependence of d_{33}^* is noted near T_{O-T} in the KNN system with a strongly linear increasing in d_{33}^* obtained in the BNBK.

9 Summary

The dielectric and piezoelectric properties of lead-free perovskites, both "past" and "present" were tabulated and compared to the family of lead base perovskites, represented by PZT. The various lead-free materials were grouped into three distinct families: (1) BaTiO$_3$; (2) (Na,Bi)Ti-BaTiO$_3$-(K,Bi)TiO$_3$ (BNBK) and (3) (K,Na)NbO3 (KNN).

Initially, the dielectric permittivity (ε_r) and piezoelectric strain coefficient d_{33} were contrasted as a function of transition temperature (T_C), whereby little intrinsic dependency was observed. The inherently low T_C of BaTiO$_3$ (T_C less than 120 °C), directed further details on the BNBK and KNN families. Analogous to PZT, a morphotropic phase boundary separating ferroelectric rhombohedral and tetragonal phases is observed in the BNBK system(s), leading to enhanced properties. However, the onset of an anti-ferroelectric phase well below the ferroelectric–paraelectric transition (T_C) results in a loss of piezoelectric activity. Furthermore, the MPB is strongly curved as compared to the PZT system. Upon examination of the relatively high T_Cs of the KNN materials (T_Cs>400 °C), they appear to be comparable to PZTs. Unfortunately, this family is plagued with the occurrence of polymorphic phase transitions as found in BaTiO$_3$ and related perovskite systems. These ferroelectric–ferroelectric phase transitions occur at temperatures far below T_C with the most piezoelectrically active

transition occurring for the orthorhombic–tetragonal transition (T_{O-T}), being $\sim$ 200 °C for pure (K,Na)NbO$_3$. Though an orthorhombic–orthorhombic MPB boundary does occur in the $(1-x)$KNbO$_3-x$NaNbO$_3$ ($x\sim$0.5), the enhancement in piezoelectric properties is modest as compared to PZT with little or no enhancement in dielectric properties. Optimized processing of these materials has yet to yield significant piezoelectric performance.

Piezoelectric properties comparable to PZTs reported for KNN materials are noted for systems where the polymorphic phase transition T_{O-T} is shifted downward near room temperature. As expected, the properties are strongly temperature dependent and thermal cycling through the two distinct domain states results in the degradation of properties.

Analogous to donor and acceptor doped PZTs, the lead-free materials were further categorized in terms of "soft" and "hard" piezoelectrics. For the BNBK family, their relatively high coercive fields (E_C>30 kV/cm) were indicative of hard piezoelectrics, but their high dielectric loss, low mechanical Qs ($\sim$100) reflected soft behavior. The addition of various dopants had little effect on the properties, with the underlying changes being related to a downward shift in the T_d and grain size effects. The orthorhombic–orthorhombic MPB based KNN materials also exhibited "soft" like behavior with high dielectric loss, and low coercive fields with $E_C\sim$5 kV/cm and low to intermediate Q values. The effect of various additives such as SnO$_2$, ZnO improved the properties, acting as a sintering aid, improving densification and/or affecting grain size. The addition of CuO, however, was found to act as an acceptor dopant, significantly increasing Q and decreasing dielectric loss.
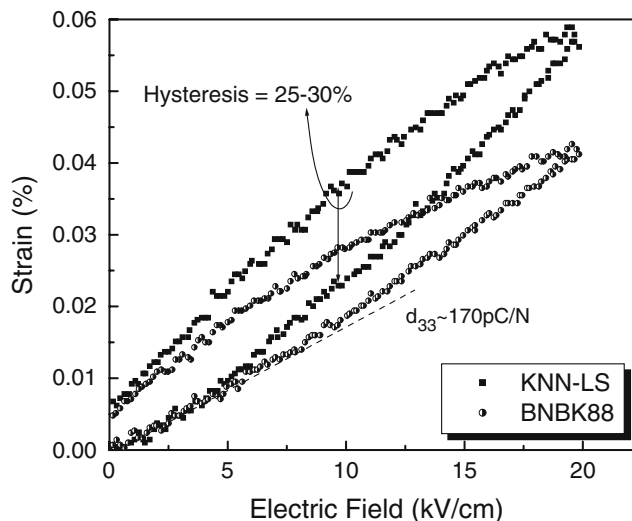

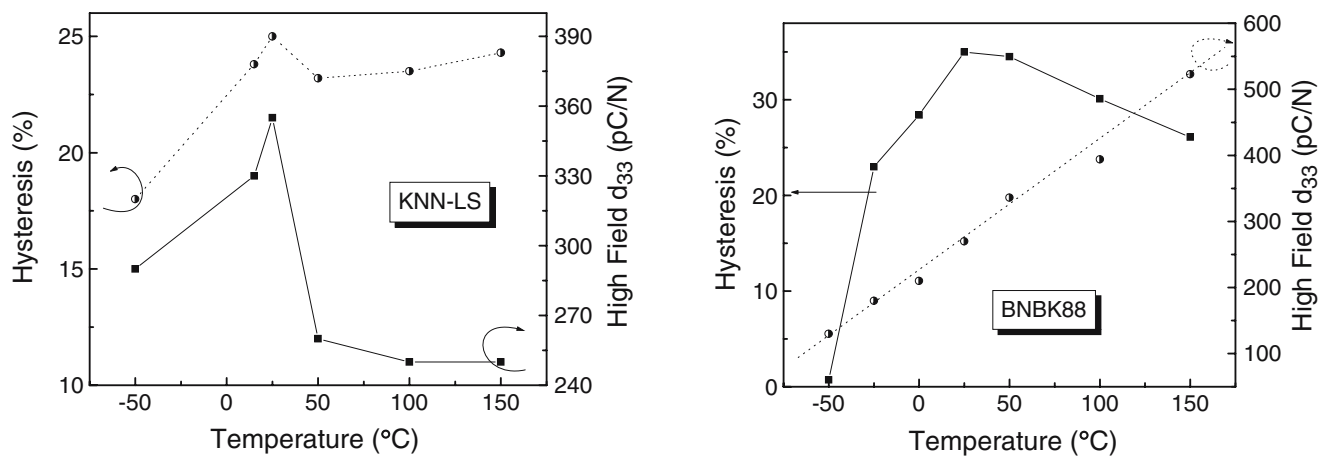Fig. 21 Unipolar strain versus electric field for lead-free piezoelectrics

Fig. 22 Strain hysteresis and high field d_{33}^* values as a function of temperature for KNN-LS (*left*) (after [63]) and BNBK88 (*right*) (after [59])

The KNN materials, compositionally engineered with their polymorphic phase transition T_{O-T} shifted to near room temperature, all exhibited soft like behavior, with low Qs. Interestingly, the coercive field of these materials was more indicative of a hard piezoelectric with E_Cs > 15 kV/cm, being also higher than unmodified KNN. Further evidence of soft behavior was found for both the BNBK and KNN materials with extrinsic contributions exemplified by strain – E field hysteresis to the levels similar to soft PZTs.

In addition to the levels of piezoelectric activity, secondary issues of property temperature dependence, temperature usage range and extrinsic response to various boundary conditions are necessary to technologically contrast the lead-free materials as they relate to various generic applications. For the case of sensors, the piezoelectric charge coefficient d_{33} and voltage coefficient g_{33} are the principle figure of merits with values for the lead-free materials being only one half to one third of "soft" PZTs, the material typically used in accelerometers and related pressure sensing devices. The need for temperature independent properties under scores the significance of the MPB based PZT compositions and its correspondingly high T_Cs, allowing operation up to temperatures above 200 °C. In contrast, the highly curved MPB of the BNBK and its low T_d and polymorphic phase transition of the KNN are

clearly inadvantageous. Applications using the converse piezoelectric effect, as for high strain actuators, require a high d_{33} and broad temperature usage range as reflected for the development of multilayer actuators used in fuel injection systems, being operational from −50 to 150 °C with high strain d_{33}s greater than 600 pC/N desired [71]. It is further evident that such devices must be stable as a function of thermal cycling.

Applications that have less constraint on transition temperature include ultrasonic transducers used in medical diagnostics. In these applications, the figure of merit in principally the longitudinal coupling square (k_{33}^2), which translate into device performance in terms of bandwidth and sensitivity. As such, the optimum lead based materials offer values nearly 50% higher. Equally important is the need for high clamped permittivity ε_r^s for electrical impedance matching of small elements in high frequency arrays, where PZT Type VI offers nearly three times the value of lead-free materials.

Finally, manufacturability plays a very important role in the implementation of materials into actual devices. For KNN, processing in an aqueous environment generally leads to issues of high dielectric loss, though recent work has shown that moisture tolerant materials can be achieved by careful processing that ensure full densification [7].

Fig. 23 SEM images for PZT (*left*) and KNN-LT (*right*) lead-free materials, showing different microstructure
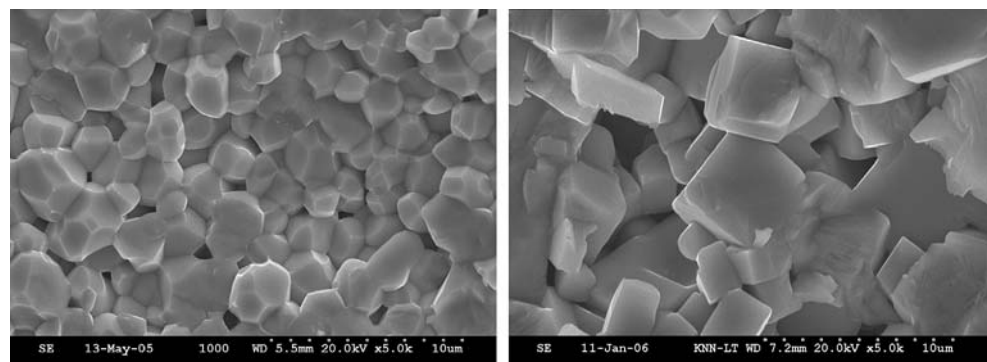
The presence of a polymorphic phase transitions and the relatively low T_d in the KNN and BNBK families, respectively, can lead to significant degradation in the peizoelectric properties upon machining of the ceramics due to both temperature and stress effects. In contrast to PZTs, the microstructures shown in Fig. 23, reflect contrasting morphologies, with nearly cubic like grains for the lead-free materials (right) as compared to the nearly dodecahedron grains of PZTs (left). The effect of the distinct microstructures on machining and mechanical properties warrants further investigations.

10 Future work

In this section, we leave the reader with a few questions:

(1) For morphotropic phase boundary systems in the BNBK family, can we eliminate or increase T_d, providing better temperature dependence and wider usage range?

(2) For the KNN family, can we shift the polymorphic phase transitions to improve temperature stability while maintaining high piezoelectric properties?

(3) For the above systems, can acceptor and donor dopants be identified for the engineering of "soft" and "hard" classes of lead-free piezoelectrics?

(4) Fundamentally, what are the role of domains and domain boundaries on the extrinsic response in these materials? Can "domain engineering" be used to enhance the properties?

For lead-free materials to be successfully implemented, investigations of manufacturability as it pertains to specific applications must be made. Examples of this are issues of electrode-ceramic interactions in co-fired multilayer actuators, depolarization during soldering, etc.

References

1. B. Jaffe, W. Cook, H. Jaffe, *Piezoelectric Ceramics* (Academic, NY, 1971), p. 92
2. D. Berlincourt, in *Ultrasonic Transducer Materials: Piezoelectric Crystals and Ceramics*, ed. By O.E. Mattiat (Plenum, London, 1971), Ch.2
3. A.J. Moulson, J.M. Herbert, *Electroceramics—Materials, Properties, Applications* (Chapman & Hall, London, 1990)
4. J.M. Herbert, *Ferroelectric Transducers and Sensors* (Gordon and Breach Science, New York, 1982)
5. Y. Saito, H. Takao, T. Tani, T. Nonoyama, K. Takatori, T. Homma, T. Nagaya, M. Nakamura, Nature **432**, 84–87 (2004)
6. E. Hollenstein, M. Davis, D. Damjanovic, N. Setter, Appl. Phys. Lett. **87**, 182905 (2005)
7. Y. Saito, H. Takao, Ferroelectrics **338**, 17–32 (2006)
8. R. Wang, R. Xie, K. Hanada, K. Matsusaki, H. Bando, M. Itoh, Phys. Status Solidi, A Appl. Res. **202**, R57–R59 (2005)
9. R. Wang, R.J. Xie, K. Hanada, K. Matsusaki, H. Bando, T. Sekiya, M. Itoh, Ferroelectrics **336**, 39–46 (2006)
10. Y. Guo, K. Kakimoto, H. Ohsato, Mater. Lett. **59**, 241–245 (2005)
11. Y. Guo, K. Kakimoto, H. Ohsato, Appl. Phys. Lett. **85**, 4121–4123 (2004)
12. G.Z. Zang, J.F. Wang, H.C. Chen, W.B. Su, C.M. Wang, P. Qi, B.Q. Ming, J. Du, L.M. Zheng, S.J. Zhang, T.R. Shrout, Appl. Phys. Lett. **88**, 212908 (2006)
13. S.B. Lang, W. Zhu, L.E. Cross, Ferroelectrics **336**, 15–21 (2006)
14. H. Takao, Y. Saito, Y. Aoki, K. Horibuchi, J. Am. Ceram. Soc. **89**, 1951–1956 (2006)
15. S. Tashiro, K. Ishii, J. Ceram. Soc. Jpn., Int. ed. **114**, 386–391 (2006)
16. Y. Saito, H. Takao, in *12th US–Japan Seminar on Dielectric and Piezoelectric Ceramics*, ed. By C. Wu, H. Kishi, C. Randall, P. Pinceloup, H. Funakubo, (Maryland, 2005), pp. 103–107
17. M. Matsubara, K. Kikuta, S. Hirano, J. Appl. Phys. **97**, 114105 (2005)
18. M. Matsubara, T. Yamaguchi, W. Sakamoto, K. Kikuta, T. Yogo, S. Hirano, J. Am. Ceram. Soc. **88**, 1190–1196 (2005)
19. J. Yoo, J. Hong, H. Lee, Y. Jeong, B. Lee, H. Song, J. Kwon, Sens. Actuators, A, Phys. **126**, 41–47 (2006)
20. S.H. Choy, X.X. Wang, H.L.W. Chan, C.L. Choy, Appl. Phys. A **82**, 715–720 (2006)
21. Y. Yuan, S. Zhang, X. Zhou, J. Liu, Jpn. J. Appl. Phys. **45**, 831–834 (2006)
22. D. Lin, D. Xiao, J. Zhu, P. Yu, Appl. Phys. Lett. **88**, 062901 (2006)
23. X.X. Wang, X.G. Tang, H.L.W. Chan, Appl. Phys. Lett. **85**, 91 (2004)
24. Y. Hiruma, R. Aoyagi, H. Nagata, T. Takenaka, Jpn. J. Appl. Phys. **43**, 7556–7559 (2004)
25. T. Takenaka, H. Nagata, Key Eng. Mater. **157–158**, 57–64 (1999)
26. T. Takenaka, H. Nagata, J. Eur. Ceram. Soc. **25**, 2693–2700 (2005)
27. S.H. Choy, X.X. Wang, H.L.W. Chan, C.L. Choy, Ferroelectrics **336**, 69–79 (2006)
28. J.S. Song, S.J. Jeong, I.S. Kim, D.S. Lee, E.C. Park, Ferroelectrics **338**, 3–8 (2006)
29. J.T. Zeng, K.W. Kwok, H.L.W. Chan, J. Am. Ceram. Soc. **89**, 2828–2832 (2006)
30. X. Wang, H.L.W. Chan, C.L. Choy, Solid State Commun. **125**, 395–399 (2003)
31. S. Zhao, G. Li, A. Ding, T. Wang, Q. Yin, J. Phys. D: Appl. Phys. **39** 2277–2281 (2006)
32. T. Takenaka, K. Maruyama, K. Sakata, Jpn. J. Appl. Phys. **30**, 2236–2239 (1991)
33. H. Nagata, M. Yoshida, Y. Makiuchi, T. Takenaka, Jpn. J. Appl. Phys. **42**, 7401–7403 (2003)
34. Y. Hiruma, Y. Makiuchi, R. Aoyagi, H. Nagata, T. Takenaka, Ceram. Trans. **174**, 139–146 (2006)
35. L. Wu, D. Xiao, D. Lin, J. Zhu, P. Yu, Jpn. J. Appl. Phys. **44**, 8515–8518 (2005)
36. D. Lin, D. Xia, J. Zhu, P. Yu, Phys. Status Solidi, A Appl. Res. **202**, R89–91 (2005)
37. R. Wang, N. Tachibana, N. Miura, K. Hanada, K. Matsusaki, H. Bando, M. Itoh, Ferroelectrics **331**, 135–139 (2006)
38. M.D. Maeder, D. Damjanovic, N. Setter, J. Electroceramics **13**, 385–392 (2004)

39. W. Chen, Y. Li, Q. Xu, J. Zhou, J. Electroceramics **15**, 229–235 (2005)
40. D. Berlincourt, in *Ultrasonic Transducer Materials: Piezoelectric Crystals* and Ceramics, ed. By O.E. Mattiat (Plenum, London, 1971), Ch.2
41. H. Jaffe, J. Am. Ceram. Soc. **41**, 494 (1958)
42. D. Schofield, R.F. Brown, Can. J. Phys. **35**, 594–607 (1957)
43. S.J. Zhang, R. Xia, T.R. Shrout, Unpublished
44. Y. Doshida, H. Kishi, Y. Hattori, A. Makiya, S. Tanaka, K. Uematsu, T. Kimura, in *12th US–Japan Seminar on Dielectric and Piezoelectric Ceramics*, ed. By C. Wu, H. Kishi, C. Randall, P. Pinceloup, H. Funakubo (Maryland, 2005), pp. 123–127
45. R.E. Jaeger, L. Egerton, J. Am. Ceram. Soc. **45**, 209–213 (1962)
46. G.H. Haertling, J. Am. Ceram. Soc. **50**, 329–330 (1967)
47. L. Egerton, D.M. Dillon, J. Am. Ceram. Soc. **42**, 438–442 (1959)
48. H. Du, Z. Li, F. Tang, S. Qu, Z. Pei, W. Zhou, Mater. Sci. Eng., B, Solid-state Mater. Adv. Technol. **131**, 83–87 (2006)
49. J.F. Li, K. Wang, B.P. Zhang, L.M. Zhang, J. Am. Ceram. Soc. **89**, 706–709, (2006)
50. B.P. Zhang, J.F. Li, K. Wang, H. Zhang, J. Am. Ceram. Soc. **89**, 1605–1609 (2006)
51. G. Arlt, D. Hennings, G. de With, J. Appl. Phys. **58**, 1619–1625, (1985)
52. R. Zuo, J. Rodel, R. Chen, L. Li, J. Am. Ceram. Soc. **89**, 2010–2015 (2006)
53. S.Y. Chu, W. Water, Y.D. Juang, J.T. Liaw, Ferroelectrics **287**, 23–33, (2003)
54. S.H. Park, C.W. Ahn, S. Nahm, J.S. Song, Jpn. J. Appl. Phys. **43**, L1072–L1074 (2004)
55. S.J. Zhang, E.F. Alberta, R.E. Eitel, C.A. Randall, T.R. Shrout, IEEE Trans. Ultrason. Ferroelectr. Freq. Control **52**, 2131–2139 (2005)
56. IEEE *Standards on Piezoelecricity*, ANSI/IEE Standard 176, 1987
57. G. Shirano, H. Danner, A. Pavlovie, R. Pepinsky, Phys. Rev. **93**, 672–673 (1954)
58. D. Berlincourt, IRE Trans. Ultrason. Eng. **PGUE-4**, 53–65 (1956)
59. S.J. Zhang, T.R. Shrout, H. Nagata, Y. Hiruma, T. Takenaka, IEEE Trans. Ultrason. Ferroelectr. Freq. Control (in press)
60. B. Lewis, L.A. Thomas, Proc. Internat. Conf. Solid State Phys., Electronics Telecommnus. Brussels **4**(Pt. 2), 883–890, (1960)
61. S. Triebwasser, Phys. Rev. **114**, 63–70 (1959)
62. S.J. Zhang, R. Xia, T.R. Shrout, *J. Electroceramics*. (in press)
63. S.J. Zhang, R. Xia, T.R. Shrout, G.Z. Zang, J.F. Wang, J. Appl. Phys. **100**, 104108 (2006)
64. N. Setter, ABC of piezoelectricity and piezoelectric materials, in *Piezoelectric Materials in Devices*, ed. By N. Setter (Lausanne, Switzerland, 2002), pp. 1–28
65. R.C. Pohanka, P.L. Smith, in *Electronic Ceramics: Properties, Devices, and Applications*, ed. By L.M. Levinson (Marcel Dekker, Inc., NY, 1987), Ch. 2
66. K. Carl, K.H. Hardtl, Ferroelectrics **17**, 473–486 (1978)
67. Y. Yuan, S. Zhang, X. Zhou, J. Liu, J. Mater. Sci. **41**, 565–567 (2006)
68. Y.J. Son, Y.G. Choi, J.C. Kwon, K.W. Cho, Y.M. Kim, S.Y. Kweon, T.H. Hong, Y.G. Lee, S.L. Ryu, M.S. Yoon, S.C. Ur, Mater. Sci. Forum **510–511**, 538–541 (2006)
69. X.P. Jiang, L.Z. Li, M. Zeng, H.L.W. Chan, Mater. Lett. **60**, 1786–1790 (2006)
70. S.J. Zhang, J. Luo, R. Xia, P.W. Rehrig, C.A. Randall, T.R. Shrout, Solid State Commun. **137**, 16–20 (2006)
71. K. Lubitz, C. Schuh, T. Steinkopf, A. Wilff, in *7th International Conference on New Actuators*, ed. By H. Borgmann (Messe Bremen GmbH, Bremen, 2000), pp. 58–61